Hindawi Publishing Corporation
International Journal of Polymer Science
Volume 2016, Article ID 1219469, 8 pages
http://dx.doi.org/10.1155/2016/1219469

Research Article

Magnetically Triggered Monodispersed Nanocomposite Fabricated by Microfluidic Approach for Drug Delivery

O. Yassine,[1] E. Q. Li,[2] A. Alfadhel,[1] A. Zaher,[3] M. Kavaldzhiev,[1] S. T. Thoroddsen,[2] and J. Kosel[1]

[1]*Computer, Electrical and Mathematical Sciences & Engineering Division, King Abdullah University of Science and Technology, P.O. Box 4700, Thuwal 23955-6900, Saudi Arabia*
[2]*Physical Sciences and Engineering Division, King Abdullah University of Science and Technology, Thuwal 23955-6900, Saudi Arabia*
[3]*School of Engineering, University of British Columbia, 3333 University Way, Kelowna, BC, Canada V1V 1V7*

Correspondence should be addressed to O. Yassine; omar.yassine@kaust.edu.sa and J. Kosel; jurgen.kosel@kaust.edu.sa

Received 19 February 2016; Revised 24 April 2016; Accepted 4 May 2016

Academic Editor: Kai Chen

Responsive microgel poly(N-isopropylacrylamide) or PNIPAM is a gel that can swell or shrink in response to external stimuli (temperature, pH, etc.). In this work, a nanocomposite gel is developed consisting of PNIPAM and magnetic iron oxide nanobeads for controlled release of liquids (like drugs) upon exposure to an alternating magnetic field. Microparticles of the nanocomposite are fabricated efficiently with a monodisperse size distribution and a diameter ranging from 20 to 500 μm at a rate of up to 1 kHz using a simple and inexpensive microfluidic system. The nanocomposite is heated through magnetic losses, which is exploited for a remotely stimulated liquid release. The efficiency of the microparticles for controlled drug release applications is tested with a solution of Rhodamine B as a liquid drug model. In continuous and pulsatile mode, a release of 7% and 80% was achieved, respectively. Compared to external thermal actuation that heats the entire surrounding or embedded heaters that need complex fabrication steps, the magnetic actuation provides localized heating and is easy to implement with our microfluidic fabrication method.

1. Introduction

Microgels are particles formed from three dimensional chains of polymers that can swell by taking up a suitable solvent below their transition temperature, called lower critical solution temperature (LCST), or shrink above the LCST by expelling this solvent [1, 2] (i.e., water with a few exceptions). The value of the LCST depends on the compositions of each gel and can vary in a wide range [3, 4]. Smart microgels have been developed that respond to stimuli like temperature [5], pH [6, 7], ionic strength [8], light [9, 10], and electrical field [11]. Due to their properties, smart microgels have been employed in different kinds of applications like sensing [12, 13], catalysis [14], drug delivery [15], bioseparation [16], and optical devices [17].

Poly(N-isopropylacrylamide) or PNIPAM microgel particles are one of the most common smart hydrogels which were first reported in 1986 [18]. They consist of hydrophilic amide groups and isopropyl hydrophobic moieties.

PNIPAM has a relatively low LCST (~32°C) [1] which can be tuned to adapt to clinical and pharmaceutical needs by the addition of comonomers to the synthesis protocol of PNIPAM [19].

Embedding magnetic nanobeads (NBs) into PNIPAM, creating magneto-thermoresponsive nanocomposites (MTNs), is particularly attractive as it can be remotely triggered by a magnetic field. In addition, the superparamagnetic behavior of those NBs ensures that they are demagnetized when no magnetic field is applied. This prevents them from agglomerating and helps in obtaining a homogeneous distribution inside the MTNs.

Several approaches have been used to fabricate magneto-thermoresponsive PNIPAM particles of micrometer and submicrometer size [20–24]. Most of those methods incorporate NBs into the gel by coating them into the gel. An

advantage of those methods is the small size of the magneto-thermoresponsive particles (few microns to submicrons in diameter). Sauzedde et al. [21] adopted a two-step method in which NBs were first absorbed in a synthetized PNIPAM, and then the MTNs with up to 30 wt% of magnetic content were obtained by a polymerization process. More recently, Purushotham et al. [25] succeeded in fabricating an MTN which is capable of releasing 15% in about 50 min using a magnetic field of 50 mT at 375 kHz. The fabrication process was a rather time consuming and complex two-step coprecipitation method.

In this work, by using a capillary microfluidic device [26], MTN particles were fabricated in a simple and fast way with high control over the size of the MTNs (ranging from few microns up to few millimeters). It also provides simple means of embedding NBs inside the particles by adjusting the flow rate [26, 27]. In addition, using microfluidic devices to generate MTNs at microscale level allows using minimal volume of ingredients with minimal losses, contamination, or waste generation [28, 29]. Finally, the recent advances in microfluidic technologies and low cost materials allow developing efficient and inexpensive devices for drug release applications [30, 31]. The concept of magnetically triggered drug release is presented in Figure 1: after being fabricated in a microfluidic system, the MTNs are collected and washed before they are loaded with a hydrophilic dye (used as a liquid drug model). Finally, the drug is released from the MTNs by applying an alternating magnetic field.

2. Methods

2.1. Fabrication of MTNs. Microfluidic systems have been widely used for biological and chemical applications, exploiting a continuous flow or flow focusing to produce continuous streams of liquid or to generate droplets [32–37]. In order to synthetize the MTNs, we use a flow focusing method, generating a (water I and water II)-in-oil ($(W + W)/O$) emulsion, in which two aqueous phases are mixed and encapsulated inside an oil stream. The polymerization process of MTNs from droplet to polymer particle form is very fast (less than two minutes).

The microfluidic devices in Figure 2(e) are designed and fabricated based on microscope glass slides and glass capillaries [28, 38]. The glass capillaries of 1 mm in diameter were heated and pulled by a microcapillary puller (P-1000, Sutter Instrument), to form tapered ends with the desired orifice sizes. The surface wettability was modified using a commercial coating agent (FluoroPel PFC 801A, Cytonix Corporation or Glaco Mirror Coat "Zero," Soft 99 Co.). Next, two tapered capillaries were bonded inside of the channel with epoxy (HP 250, ITW Devcon, Inc.) with one of them just penetrating the opening of the other one. Finally a glass slide working as the cover of the microfluidic device was bonded onto the channel and syringe needles were bonded to holes to form inlets.

To generate monodispersed ($(W + W)/O$) emulsions, liquid 1, liquid 2, and liquid 3 were used as the inner, middle, and outer phases, respectively. Liquid 1 contained 20 wt% of the monomer N-isopropylacrylamide (NIPAM), 2 mL of N,N,N′,N′-tetramethylenediamine (TEMED) as the accelerator for the reaction, 6 wt% of the crosslinker, N,N-methylene(bis)acrylamide (BIS), and 0.5 mL [2-(methacryloyloxy)ethyl]trimethylammonium chloride (METAC). Liquid 2 contained 4 wt% ammonium persulfate (APS) and the iron oxide NBs. Silicon oil was used as the oil phase. All chemicals were obtained from Sigma-Aldrich and the NBs (20 nm) were from Micromod (Catalog number 79-00-201).

As shown in Figure 2(a), liquid 1 was fed into the channel through the first capillary meeting liquid 2 at the outlet of the first capillary; as shown in Figure 2(b) the microfluidic approach ensures laminar flows, preventing the two liquids to mix in the second capillary, which would block it. When the two streams of liquid 1 and liquid 2 reach the outlet of the second capillary, the shear stress from liquid 3 pinches off the streams into monodispersed droplets, as shown in Figure 2(c). Figure 2(d) shows MTNs particles with PDI index value of 3.9%, indicating highly monodisperse MTNs generation in our device. Figures 2(d) and 2(e) show different sizes of MTN particles. The MTNs are collected in a glass container and washed 3 times.

2.2. Characterization of MTNs

2.2.1. Swelling/Shrinking Ratio. The thermoresponsive behavior of the MTNs was characterized by measuring the swelling/deswelling ratio:

$$\mathrm{SR} = \frac{(W_W - W_d)}{W_d}, \tag{1}$$

where W_W is the weight of the wet particles and W_d is the dry weight of the particles [39, 40]. The wet weight of the sample was measured gravimetrically. A filter paper was used to remove any excess water. The dry weight was measured after drying the sample in vacuum. We should mention that, for all the graphs and data, we used $\mathrm{SR}_{(\mathrm{normalized})}$ which was normalized according to SR value at room temperature.

2.2.2. Drug Loading. The drug model used in our work is Rhodamine B (Rh(B)), which is a hydrophilic dye (excitation/emission wavelengths = 543/620 nm). MTNs were immersed in water with 1 mg mL^{-1} of Rh(B) for 3 days at room temperature, to load the dye into the gel network by physical diffusion. The loaded MTNs were then washed twice with DI water and kept in water at room temperature for release experiments. The loading efficiency was defined as

$$\mathrm{Load}_{\mathrm{eff}} = \frac{(\text{initial Rh (B)} - \text{remaining Rh (B)})}{\text{initial amount of Rh (B)}} \times 100. \tag{2}$$

The experimental values of $\mathrm{Load}_{\mathrm{eff}}$ were obtained by measuring the amount of Rh(B) evaluated by UV spectroscopy of the water/Rh(B) solution that were sampled before and after the loading procedure.

2.2.3. Drug Release. To produce the magnetic stimuli, an alternating magnetic field (AMF) was applied using an inductive heater (Induktive Erwärmungsanlagen GmbH, Austria,

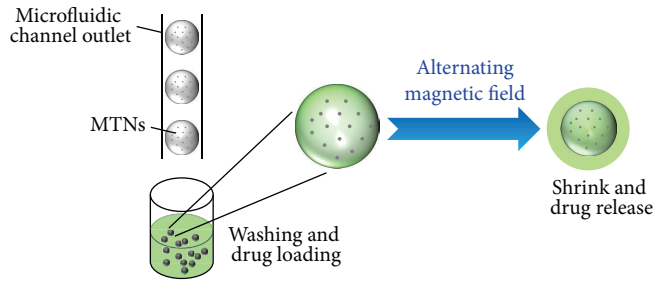

Figure 1: Principle of magnetically controlled drug release using PNIPAM microparticles with embedded iron oxide nanobeads (NBs) to form monodispersed magneto-thermoresponsive nanocomposites (MTNs). The MTNs are fabricated in a microfluidic system and filled with a drug by means of diffusion. The heat generated by the NBs upon the application of an alternating magnetic field causes the gel-structure to shrink and the release of drug.

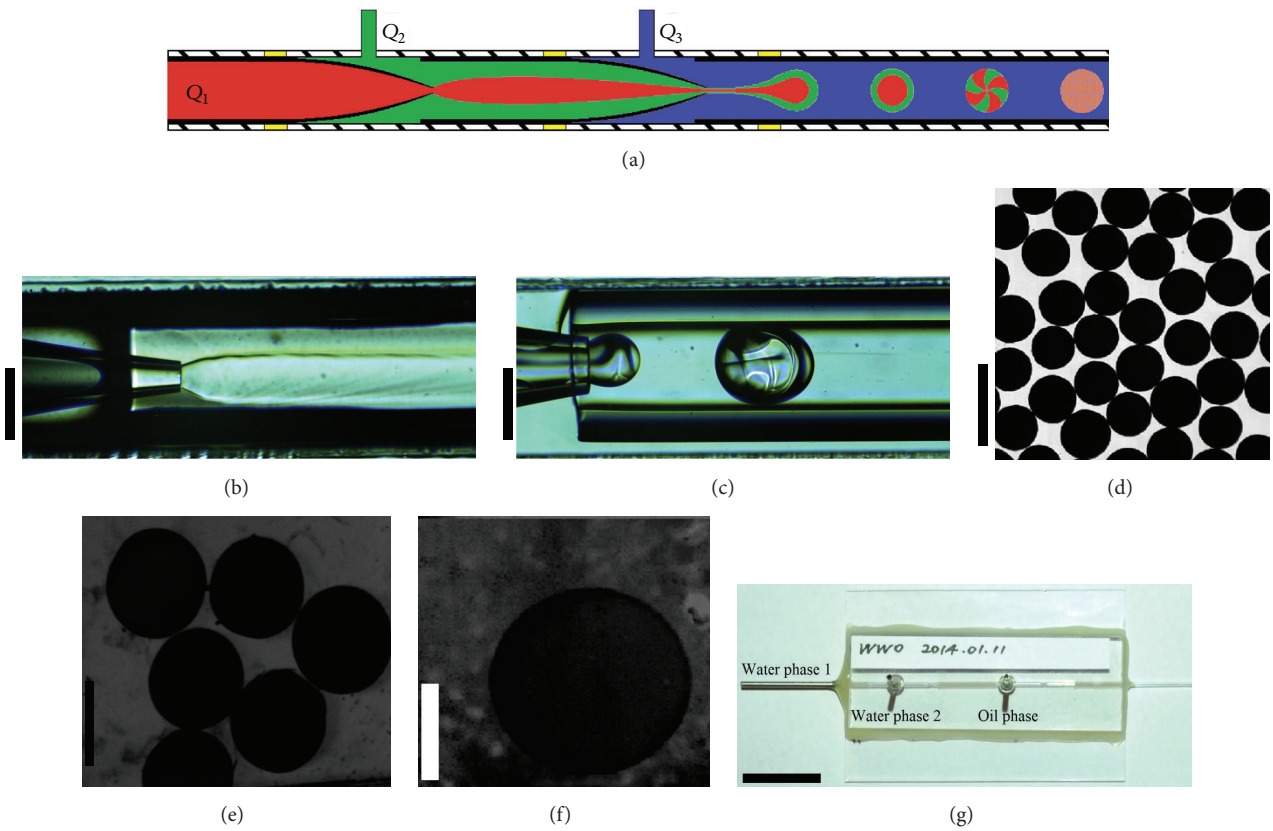

Figure 2: (a) Schematic configuration of the microfluidic system for synthetizing the MTNs. Q_1 (20 μL min^{-1}), Q_2 (20 μL min^{-1}), and Q_3 (120 μL min^{-1}) are the flow rates for the inner, middle, and outer phases, respectively. (b) The two aqueous phases meet and form a continuous laminar flow at the outlet of the first capillary. (c) The generation of $((W + W)/O)$ emulsions at the outlet of the second capillary. (d), (e), and (f) Magnified picture of different sizes (200, 100, and 20 μm) of magneto-thermoresponsive nanocomposites (MTNs) fabricated with the capillary microfluidic device. (g) A typical microfluidic device fabricated for preparing the MTNs. Scale bars are 400 μm in (b), (c), and (d), 100 μm in (e), 10 μm in (f), and 2 cm in (g).

model number TH3HT) that produces a magnetic field of 600 kHz and 72 mT. The inductive heater was connected to a chiller system to prevent heating of the coil. For the AMF experiments, the particles were placed inside a plastic container at the center of the coil and the container was insulated by a Polydimethylsiloxane (PDMS) cover [41, 42]. For the release experiments, a precise amount of MTNs water was placed in a flask containing water. The amount of Rh(B) released from the MTNs at different times in the experiment was determined by sampling precise amount of the solution before and after applying the AMF, using UV spectroscopy.

2.2.4. Theoretical Model. The heat generated by the superparamagnetic NBs, when exposed to an alternating magnetic field, is a result of magnetic losses that occur due to two mechanisms: Neel relaxation and Brownian relaxation.

Neel relaxation, τ_N, is associated with the reorientation of magnetic moments, whereas Brownian relaxation, τ_B, is associated with the reorientation of the entire particles. Neel relaxation can be expressed as [43]

$$\tau_N = \tau_0 \exp\left(\frac{KV_m}{k_B T}\right), \tag{3}$$

where τ_0 is the initial relaxation time, K is the magnetic anisotropy constant, V_m is the volume of the magnetic particle, k_B is the Boltzmann constant, and T is the temperature.

Brownian relaxation is expressed as

$$\tau_B = \frac{3\eta V_H}{k_B T}, \tag{4}$$

where η is the medium viscosity and V_H is the hydrodynamic volume of the magnetic particle.

The volumetric power dissipated by NBs is proportional to the internal energy of the particles ΔU and the frequency f and can be expressed as [44]

$$P = f\Delta U = \pi\mu_0\chi_i f H^2, \tag{5}$$

where H is the magnetic field amplitude, μ_0 is the permeability of free space, and χ_i is the imaginary part of the complex susceptibility, which depends on the frequency and Brownian and Neel relaxations. Equation (5) shows that increasing the frequency or the magnetic field amplitude results in increasing the amount of power dissipated and, hence, more heat generated inside the MTNs.

χ_i is dependent on the frequency, effective relaxation τ, and the static susceptibility $\chi_0 = \partial M/\partial H$ (which is obtained from the magnetization curves of the NBs):

$$\chi_i = \frac{2\pi f\tau}{1 + (2\pi f\tau)^2}\chi_0, \tag{6}$$

where the effective relaxation time τ is calculated as

$$\frac{1}{\tau} = \frac{1}{\tau_N} + \frac{1}{\tau_B}. \tag{7}$$

The volumetric power dissipation of MTNs with different NB volume ratio was calculated for an alternating magnetic field of 72 mT amplitude and frequency of 600 kHz. The calculation was conducted using $K = 13.5\,\mathrm{kJ\,m^{-3}}$, $\tau_0 = 1$ ns, and PNIPAM viscosity $\eta = 2.2$ mPa·s. The total power dissipated inside an MTN was calculated using (5), and the power density was derived taking into account the temperature dependent volume of the MTN (see Section 3).

3. Results and Discussion

The size of the MTNs fabricated by the microfluidic chip method ranged from 20 to 500 μm. All results reported here were achieved with MTNs of 100 μm in diameter and a NB concentration of 10 mg/mL, unless cited otherwise.

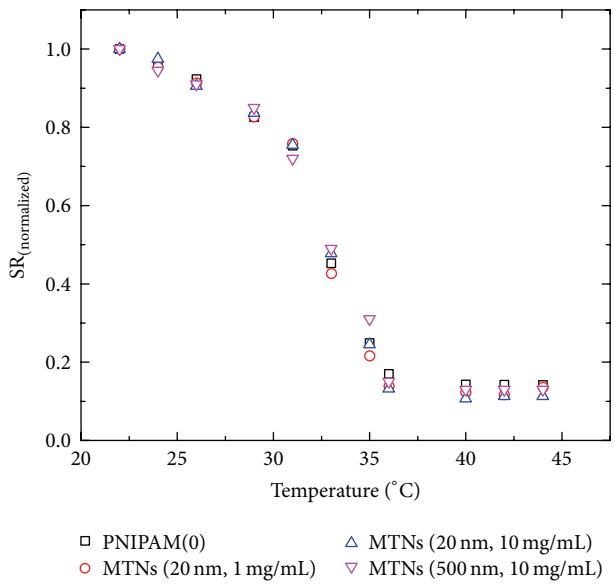

Figure 3: Swelling/deswelling ratio (normalized) of pure PNIPAM microparticles (PNIPAM(0)) and different compositions of magneto-thermoresponsive nanocomposites (MTNs). The experiments were performed by direct heating; that is, the microparticles were immersed in a water bath of controllable temperature.

3.1. Thermoresponsive Behavior. In order to study the effect of embedding the NBs into PNIPAM, we compared the swelling-deswelling behavior of native PNIPAM (PNIPAM(0)) microparticles to that of MTNs with different NBs sizes (nm in diameter) and concentrations (in $\mathrm{mg\,mL^{-1}}$). Experiments were performed with MTNs inside a water bath that enabled temperature control from 22°C to 45°C. All measurement points were recorded after the temperature reached a steady state (constant value for at least 15 minutes). Figure 3 shows the SR (normalized) of the different microparticles as a function of the temperature. An identical behavior is observed for PNIPAM(0) and MTNs, independent of the NBs concentrations and sizes. This implies that integrating magnetic nanoparticles in the PNIPAM microgel with this microfluidic fabrication method leaves its thermoresponsive behavior unchanged. This is in contrast to results obtained with chemical synthesis methods, where the nanoparticles are chemically linked and attached to the gel network, causing a decrease in the sensitivity of PNIPAM to thermal stimuli. It seems, by using the microfluidic approach for the fabrication, that the NBs are more physically linked to the gel network, maintaining efficiently the responsive behavior of the MTNs [26]. This property could be exploited to generate a variety of PNIPAM microparticles with embedded nanobeads of different kind, size, or concentration, which are optimized for specific applications. From the SR plot in Figure 3, the LCST can be estimated [45] to be around 31°C, which is in accordance with typical values reported in literature [1, 16, 46, 47].

Figure 3 shows that different ratios and compositions of NBs do not considerably affect the responsive behavior of the MTNs. The exception of this was the concentration of

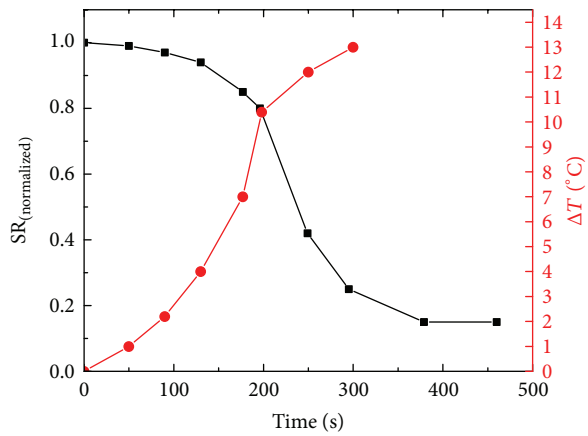

FIGURE 4: Swelling/deswelling ratio (normalized) of MTNs as a response to an alternating magnetic field (AMF) (black). The sharp decrease at around 200 seconds corresponds to the time at which the LCST is reached. Temporal variation of the average temperature of the particle caused by the heat produced in the NBs, when the AMF is on (red).

the crosslinker, which has been shown to have a direct impact on the response of MTNs.

3.2. Magneto-Thermoresponsive Behavior. To study the response of MTNs to magnetic stimuli, an alternating magnetic field (AMF) of 72 mT in amplitude and 600 kHz in frequency was applied and the SR was measured.

Figure 4 shows the normalized SR (black curve), in addition to the temporal variation (red curve) as a function of AMF duration. For the SR measurement, a slight decrease can be observed during the first two minutes, followed by a sharp decrease at around 200 seconds, before the SR saturates after about 400 seconds. Overall, the magneto-responsive behavior of the MTNs is very similar to the one obtained from direct thermal stimuli (Figure 3). The results show that the LCST of MTNs occurred about 200 seconds after applying the AMF. The maximum shrinking obtained after around 400 seconds is close to values found in other works intended specifically to increase the responsive behavior of PNIPAM microparticles [48].

From the results obtained by direct thermal stimuli (Figure 3) and magnetic stimuli (Figure 4), the average temperature change ΔT of the MTNs, when heated by an AMF, can be derived. This temperature change is shown in Figure 4 (red curve). When the MTN shrinks due to increasing temperature, its volume decreases while the number of NBs remains the same. Hence, the heating power remains the same, resulting in an increase of the power density. As a result, a nonlinear temperature change is observed.

3.3. Drug Release. Loading the MTNs with Rh(B) by physical diffusion yielded a value for the Load_{eff} of 15%. The drug release was studied for a continuous mode; that is, an AMF was continuously applied for a specific period of time and for a pulsatile mode; that is, an AMF was sequentially applied with a break between the pulses.

3.3.1. Continuous Release Mode. The temporal behavior of the release in continuous mode is shown in Figure 5(a). It closely correlates with the shrinking and temperature change of the MTNs (Figure 4). As the temperature increases and the MTNs shrink, the dye is released. Before about 3 minutes, that is, before reaching the LCST, the release is slow and reaches a value of 2%. A sharp increase of the release profile is observed around the LCST, where the MTNs shrink dramatically and the gel starts to collapse, acting like a hydrostatic pump that pushes the dye outside. After about 5 minutes, the release had a significant slowdown at 7%. About one minute later, when shrinking is completed, the pores decrease or even close, and the temperature of the MTNs does not change anymore. We should note that the magnetic field was applied for 90 minutes but data in Figure 5(a) are shown until 30 minutes only, since the release has a significant slowdown (the magnetic effect was nearly saturated, and the very slow increase beyond that is due to normal diffusion which as indicates the graph is very slow). The graph shows also the release of Rh(B) from PNIPAM particles without magnetic contents, PNIPAM(0), where the release, which is much lower than those from MTNs, is mostly due to simple diffusion.

The effect of the concentration of NBs in the MTNs on the release under magnetic stimuli is shown in Figure 5(b). In general, a higher concentration of NBs yields a higher temperature of the MTNs, resulting in a larger release. Below 4 mg mL^{-1}, no release was observed, which is attributed to the fact that the heating of the MTNs is not sufficient to generate a response. Between 4 mg mL^{-1} and 6.5 mg mL^{-1}, the release is small with values below 2%. Between 6.5 and 10 mg mL^{-1}, the release increases linearly from about 2% to about 7.5%. Within this concentration range, the temperature reaches the LCST, causing an increased release due to pronounced shrinking. While maximum shrinking is obtained with a concentration of 10 mg mL^{-1}, the release continues to increase, though slower, with the concentration. This effect is generated by the increasing temperature inside the MTNs that is driving the release. This indicates that it would be possible to increase the release beyond 7.5% by further increasing the NBs concentration; however, in our experiments we found that the polymerization of the gel was affected at such high concentrations.

3.3.2. Pulsatile Release Mode. The release can be enhanced by a pulsatile release profile, which is also important for applications that need a successive release of drug such as the release of insulin [49]. The pulsatile release mode was studied by applying AMF pulses of 6-minute duration separated by 5-minute intervals without magnetic field. The pulse duration was chosen to obtain a maximum release as found in the continuous release mode. As shown in Figure 5(c), the MTNs maintain a relatively constant release for each pulse even after 15 cycles, and a total release of nearly 80% was achieved within 1.5 hours. The reason for the increased release performance is that unlike the continuous AMF mode (where the gel can collapse, leading to a decrease of the pore dimensions or even clogging of the pores) the pulsatile mode enables the gel to reswell, resulting in an opening of the pores for the next cycle.

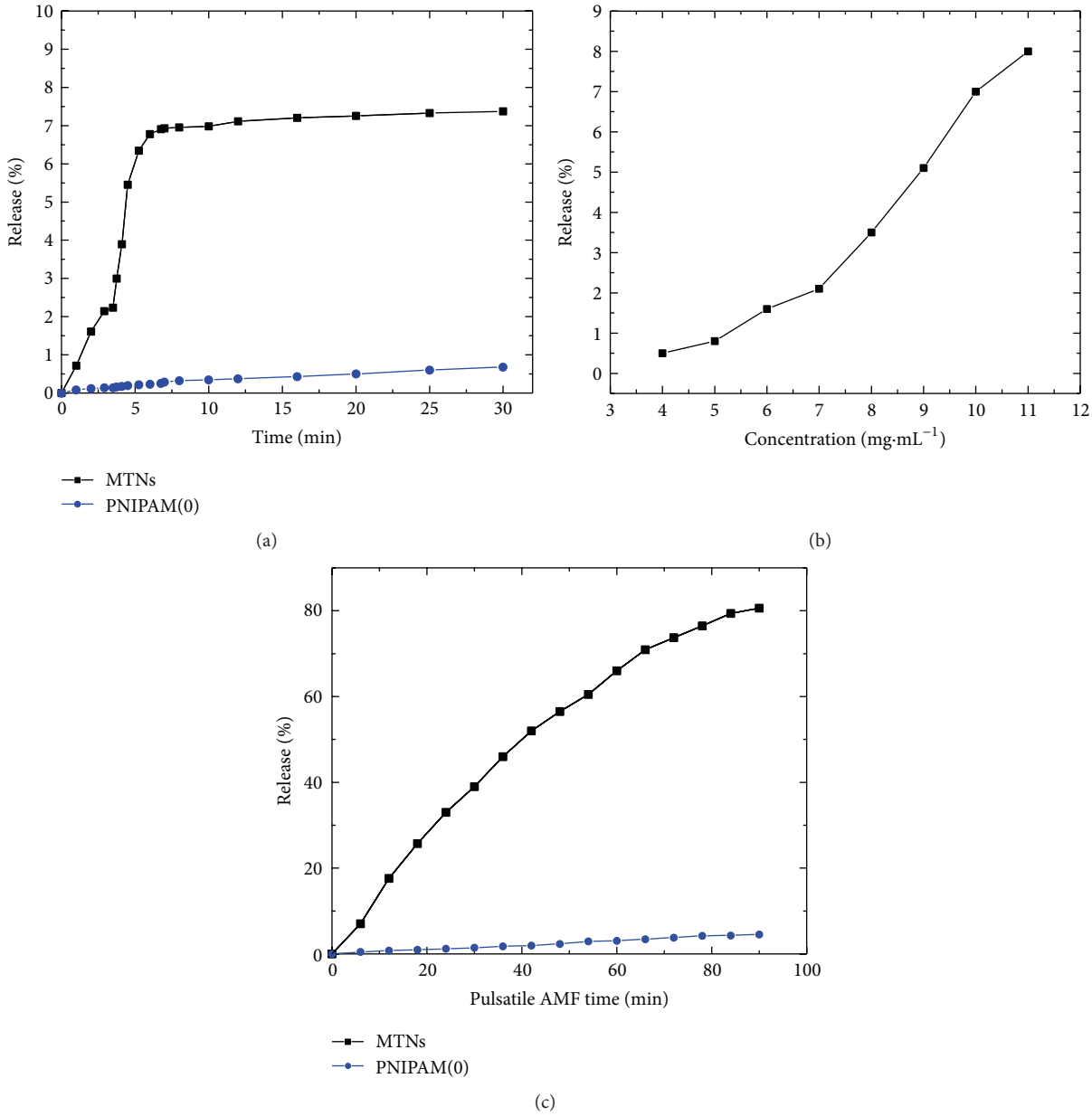

Figure 5: (a) Release rate of Rh(B) from MTNs and PNIPAM(0) when an AMF is applied continuously for 30 minutes. (b) Effect of iron oxide nanobeads (NBs) concentration on the release rate of Rh(B) after applying magnetic stimuli for 7 minutes. (c) Pulsatile release of Rh(B) from MTNs and PNIPAM(0) by consecutively applying an alternating magnetic field (AMF) for 6 minutes separated by 5-minute intervals without magnetic field.

Similarly to Figure 5(a), release of Rh(B) from PNIPAM(0), which is mainly due to simple diffusion, was presented and used as control test to show the significant effect of magnetic triggering (case of MTNs).

4. Conclusions

In this work, PNIPAM microparticles with embedded NBs were studied for controlled release applications. The fabrication of monodispersed MTNs was performed using a capillary microfluidic system, providing a versatile, simple, and fast method to produce MTNs from 20 to 500 μm in diameter at a rate of up to 1 kHz. The produced MTNs have a temperature behavior that is characterized by the LCST at 31°C.

The drug release study was carried out by remotely triggering the MTNs with an AMF of 72 mT in amplitude and 600 kHz in frequency. It is found that the MTNs are able to deswell by more than 80% of their initial weight within a short time (around 6 minutes) under the effect of an AMF.

We found that the thermoresponsive behavior of the MTNs is not affected by the NB size and concentration up to 500 nm and 10 mg mL^{-1}, respectively. This seems to

be a distinct feature of the developed fabrication process, offering a high flexibility in the choice of the embedded particles. Beyond 10 mg mL^{-1}, the polymerization got adversely affected. On the other hand the crosslinker concentration has a considerable effect and more than 2.5 wt% should be used to achieve the maximum responsive behavior. The experiments also showed that increasing the concentration of NBs increases the amount of drug release. This could be linked to the saturation temperature of the MTNs, which increases with the NB concentration. The efficiency of the particles for drug release applications was shown using Rh(B) as a model of liquid drugs. In case of a continuous application of the AMF, a release of nearly 7% was achieved in 7 minutes. Thereby, the release rate closely correlates with the shrinking and temperature increase of the MTNs. In case of pulsatile application of the AMF nearly 80% of release was obtained within 100 minutes.

Competing Interests

The authors declare that they have no competing interests.

Acknowledgments

Research reported in this publication was supported by King Abdullah University of Science and Technology (KAUST). E. Q. Li is grateful for a SABIC Postdoctoral Fellowship.

References

[1] Y. Hirokawa and T. Tanaka, "Volume phase transition in a nonionic gel," *The Journal of Chemical Physics*, vol. 81, no. 12, pp. 6379–6380, 1984.

[2] B. R. Saunders and B. Vincent, "Microgel particles as model colloids: theory, properties and applications," *Advances in Colloid and Interface Science*, vol. 80, no. 1, pp. 1–25, 1999.

[3] K. Suwa, K. Morishita, A. Kishida, and M. Akashi, "Synthesis and functionalities of poly(*N*-vinylalkylamide). V. Control of a lower critical solution temperature of poly(*N*-Vinylalkylamide)," *Journal of Polymer Science, Part A: Polymer Chemistry*, vol. 35, no. 15, pp. 3087–3094, 1997.

[4] C.-K. Chee, B. J. Hunt, S. Rimmer, R. Rutkaite, I. Soutar, and L. Swanson, "Manipulating the thermoresponsive behaviour of poly(N-isopropylacrylamide) 3. on the conformational behaviour of N-isopropylacrylamide graft copolymers," *Soft Matter*, vol. 5, no. 19, pp. 3701–3712, 2009.

[5] S.-K. Ahn, R. M. Kasi, S.-C. Kim, N. Sharma, and Y. X. Zhou, "Stimuli-responsive polymer gels," *Soft Matter*, vol. 4, no. 6, pp. 1151–1157, 2008.

[6] B. R. Saunders, H. M. Crowther, and B. Vincent, "Poly[(methyl methacrylate)-co-(methacrylic acid)] microgel particles: swelling control using pH, cononsolvency, and osmotic deswelling," *Macromolecules*, vol. 30, no. 3, pp. 482–487, 1997.

[7] S. Dai, P. Ravi, and K. C. Tam, "pH-responsive polymers: synthesis, properties and applications," *Soft Matter*, vol. 4, no. 3, pp. 435–449, 2008.

[8] L. Hu and M. J. Serpe, "The influence of deposition solution ph and ionic strength on the quality of poly(*N*-isopropylacrylamide) microgel-based thin films and etalons," *ACS Applied Materials and Interfaces*, vol. 5, no. 22, pp. 11977–11983, 2013.

[9] A. Garcia, M. Marquez, T. Cai et al., "Photo-, thermally, and pH-responsive microgels," *Langmuir*, vol. 23, no. 1, pp. 224–229, 2007.

[10] Z. Zhu, E. Senses, P. Akcora, and S. A. Sukhishvili, "Programmable light-controlled shape changes in layered polymer nanocomposites," *ACS Nano*, vol. 6, no. 4, pp. 3152–3162, 2012.

[11] A. Fernández-Nieves, A. Fernández-Barbero, F. J. de las Nieves, and B. Vincent, "Motion of microgel particles under an external electric field," *Journal of Physics Condensed Matter*, vol. 12, no. 15, pp. 3605–3614, 2000.

[12] T. Hoare and R. Pelton, "Engineering glucose swelling responses in poly(N-isopropylacrylamide)-based microgels," *Macromolecules*, vol. 40, no. 3, pp. 670–678, 2007.

[13] R. E. Rivero, M. A. Molina, C. R. Rivarola, and C. A. Barbero, "Pressure and microwave sensors/actuators based on smart hydrogel/conductive polymer nanocomposite," *Sensors and Actuators, B: Chemical*, vol. 190, pp. 270–278, 2014.

[14] A. Pich, J. Hain, Y. Lu, V. Boyko, Y. Prots, and H.-J. Adler, "Hybrid microgels with ZnS inclusions," *Macromolecules*, vol. 38, no. 15, pp. 6610–6619, 2005.

[15] R. F. Donnelly, M. T. C. McCrudden, A. Z. Alkilani et al., "Hydrogel-forming microneedles prepared from 'super swelling' polymers combined with lyophilised wafers for transdermal drug delivery," *PLoS ONE*, vol. 9, no. 10, Article ID e111547, 2014.

[16] K. Nagase, J. Kobayashi, and T. Okano, "Temperature-responsive intelligent interfaces for biomolecular separation and cell sheet engineering," *Journal of The Royal Society Interface*, vol. 6, supplement 3, p. S293, 2009.

[17] L. Dong, A. K. Agarwal, D. J. Beebe, and H. R. Jiang, "Adaptive liquid microlenses activated by stimuli-responsive hydrogels," *Nature*, vol. 442, no. 7102, pp. 551–554, 2006.

[18] R. H. Pelton and P. Chibante, "Preparation of aqueous latices with N-isopropylacrylamide," *Colloids and Surfaces*, vol. 20, no. 3, pp. 247–256, 1986.

[19] R. X. Liu, M. Fraylich, and B. R. Saunders, "Thermoresponsive copolymers: from fundamental studies to applications," *Colloid and Polymer Science*, vol. 287, no. 6, pp. 627–643, 2009.

[20] R. Regmi, S. R. Bhattarai, C. Sudakar et al., "Hyperthermia controlled rapid drug release from thermosensitive magnetic microgels," *Journal of Materials Chemistry*, vol. 20, no. 29, pp. 6158–6163, 2010.

[21] F. Sauzedde, A. Elaïssari, and C. Pichot, "Hydrophilic magnetic polymer latexes. 2. Encapsulation of adsorbed iron oxide nanoparticles," *Colloid and Polymer Science*, vol. 277, no. 11, pp. 1041–1050, 1999.

[22] X. B. Ding, Z. H. Sun, G. X. Wan, and Y. Y. Jiang, "Preparation of thermosensitive magnetic particles by dispersion polymerization," *Reactive and Functional Polymers*, vol. 38, no. 1, pp. 11–15, 1998.

[23] S. Purushotham and R. V. Ramanujan, "Thermoresponsive magnetic composite nanomaterials for multimodal cancer therapy," *Acta Biomaterialia*, vol. 6, no. 2, pp. 502–510, 2010.

[24] S. R. Deka, A. Quarta, R. Di Corato, A. Riedinger, R. Cingolani, and T. Pellegrino, "Magnetic nanobeads decorated by thermoresponsive PNIPAM shell as medical platforms for the efficient delivery of doxorubicin to tumour cells," *Nanoscale*, vol. 3, no. 2, pp. 619–629, 2011.

[25] S. Purushotham, P. E. J. Chang, H. Rumpel et al., "Thermoresponsive core-shell magnetic nanoparticles for combined modalities of cancer therapy," *Nanotechnology*, vol. 20, no. 30, Article ID 305101, 2009.

[26] J.-W. Kim, A. S. Utada, A. Fernández-Nieves, Z. B. Hu, and D. A. Weitz, "Fabrication of monodisperse gel shells and functional microgels in microfluidic devices," *Angewandte Chemie—International Edition*, vol. 46, no. 11, pp. 1819–1822, 2007.

[27] Y. L. Yu, M. J. Zhang, R. Xie et al., "Thermo-responsive monodisperse core-shell microspheres with PNIPAM core and biocompatible porous ethyl cellulose shell embedded with PNIPAM gates," *Journal of Colloid and Interface Science*, vol. 376, no. 1, pp. 97–106, 2012.

[28] L. Y. Chu, J. W. Kim, R. K. Shah, and D. A. Weitz, "Monodisperse thermoresponsive microgels with tunable volume-phase transition kinetics," *Advanced Functional Materials*, vol. 17, no. 17, pp. 3499–3504, 2007.

[29] S. Prakash and J. Yeom, *Nanofluidics and Microfluidics*, William Andrew Publishing, 2014.

[30] I. V. Zhigaltsev, Y. K. Tam, A. K. K. Leung, and P. R. Cullis, "Production of limit size nanoliposomal systems with potential utility as ultra-small drug delivery agents," *Journal of Liposome Research*, vol. 26, no. 2, pp. 96–102, 2016.

[31] J. S. Kochhar, S. Y. Chan, P. S. Ong, W. G. Lee, and L. Kang, "Microfluidic devices for drug discovery and analysis," in *Microfluidic Devices for Biomedical Applications*, X.-J. J. Li and Y. Zhou, Eds., chapter 7, pp. 231–280, Woodhead, Cambridge, UK, 2013.

[32] C. P. Gooneratne, O. Yassine, I. Giouroudi, and J. Kosel, "Selective manipulation of superparamagnetic beads by a magnetic microchip," *IEEE Transactions on Magnetics*, vol. 49, no. 7, pp. 3418–3421, 2013.

[33] L. Renaud, O. Yassine, P. Kleimann et al., "Electrophoresis poly(dimethylsiloxane)/glass chips with integrated active cooling for quantification of amino acids," *Experimental Heat Transfer*, vol. 23, no. 1, pp. 63–72, 2010.

[34] O. Yassine, P. Morin, O. Dispagne et al., "Electrophoresis PDMS/glass chips with continuous on-chip derivatization and analysis of amino acids using naphthalene-2,3-dicarboxaldehyde as fluorogenic agent," *Analytica Chimica Acta*, vol. 609, no. 2, pp. 215–222, 2008.

[35] K. Faure, M. Blas, O. Yassine et al., "Electrochromatography in poly(dimethyl)siloxane microchips using organic monolithic stationary phases," *Electrophoresis*, vol. 28, no. 11, pp. 1668–1673, 2007.

[36] A. Alfadhel, B. Li, A. Zaher, O. Yassine, and J. Kosel, "A magnetic nanocomposite for biomimetic flow sensing," *Lab on a Chip—Miniaturisation for Chemistry and Biology*, vol. 14, no. 22, pp. 4362–4369, 2014.

[37] O. Yassine, C. P. Gooneratne, D. Abu Smara et al., "Isolation of cells for selective treatment and analysis using a magnetic microfluidic chip," *Biomicrofluidics*, vol. 8, no. 3, Article ID 034114, 2014.

[38] E. Q. Li, J. M. Zhang, and S. T. Thoroddsen, "Simple and inexpensive microfluidic devices for the generation of monodisperse multiple emulsions," *Journal of Micromechanics and Microengineering*, vol. 24, no. 1, Article ID 015019, 2014.

[39] E. Vallés, D. Durando, I. Katime, E. Mendizábal, and J. E. Puig, "Equilibrium swelling and mechanical properties of hydrogels of acrylamide and itaconic acid or its esters," *Polymer Bulletin*, vol. 44, no. 1, pp. 109–114, 2000.

[40] P. F. Liu, J. Peng, J. Q. Li, and J. L. Wu, "Radiation crosslinking of CMC-Na at low dose and its application as substitute for hydrogel," *Radiation Physics and Chemistry* , vol. 72, no. 5, pp. 635–638, 2005.

[41] B. Li, O. Yassine, and J. Kosel, "A surface acoustic wave passive and wireless sensor for magnetic fields, temperature, and humidity," *IEEE Sensors Journal*, vol. 15, no. 1, pp. 453–462, 2014.

[42] B. Li, O. Yassine, and J. Kosel, "Integrated passive and wireless sensor for magnetic fields, temperature and humidity," in *Proceedings of the 12th IEEE SENSORS*, pp. 1–4, Baltimore, Md, USA, November 2013.

[43] W. F. Brown Jr., "Thermal fluctuations of a single-domain particle," *Physical Review*, vol. 130, no. 5, pp. 1677–1686, 1963.

[44] R. E. Rosensweig, "Heating magnetic fluid with alternating magnetic field," *Journal of Magnetism and Magnetic Materials*, vol. 252, pp. 370–374, 2002.

[45] H. G. Schild, "Poly(*N*-isopropylacrylamide): experiment, theory and application," *Progress in Polymer Science*, vol. 17, no. 2, pp. 163–249, 1992.

[46] M. E. Nash, D. Healy, W. M. Carroll, C. Elvira, and Y. A. Rochev, "Cell and cell sheet recovery from pNIPAm coatings; motivation and history to present day approaches," *Journal of Materials Chemistry*, vol. 22, no. 37, pp. 19376–19389, 2012.

[47] Y. W. Zhang, M. Jiang, J. X. Zhao, X. W. Ren, D. Y. Chen, and G. Z. Zhang, "A novel route to thermosensitive polymeric core-shell aggregates and hollow spheres in aqueous media," *Advanced Functional Materials*, vol. 15, no. 4, pp. 695–699, 2005.

[48] L.-W. Xia, R. Xie, X.-J. Ju, W. Wang, Q. M. Chen, and L.-Y. Chu, "Nano-structured smart hydrogels with rapid response and high elasticity," *Nature Communications*, vol. 4, article 2226, 2013.

[49] S. Sershen and J. West, "Corrigendum to: "Implantable, polymeric systems for modulated drug delivery": [Advanced Drug Delivery Reviews 54 (2002) 1225–1235]," *Advanced Drug Delivery Reviews*, vol. 55, no. 3, p. 439, 2003.